# Figure 5 Saito et al.

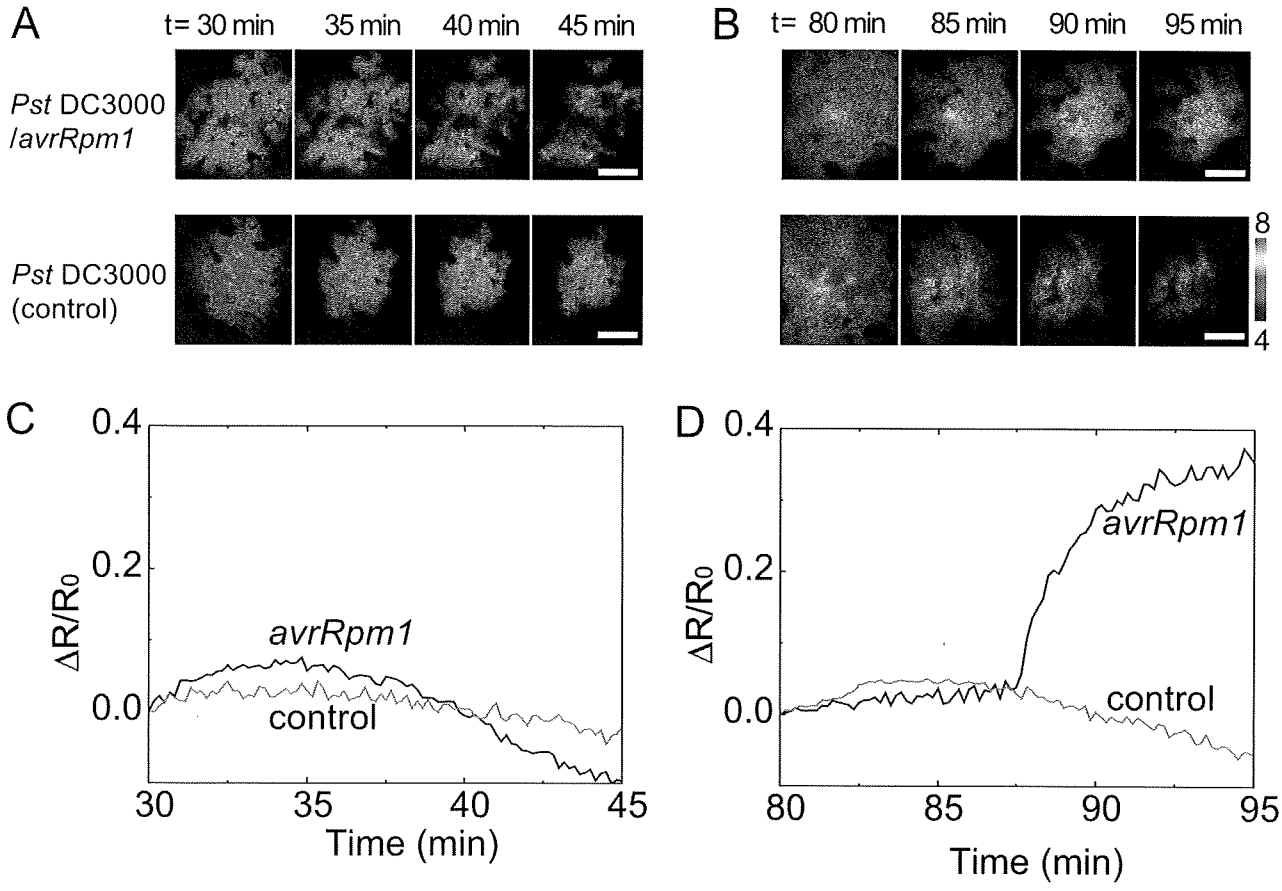

# An ultramarine fluorescent protein with increased photostability and pH insensitivity

Wataru Tomosugi[1], Tomoki Matsuda[1], Tomomi Tani[1], Tomomi Nemoto[2], Ippei Kotera[1], Kenta Saito[3], Kazuki Horikawa[3] & Takeharu Nagai[1,3]

**We report a pH-insensitive and photostable ultramarine fluorescent protein, Sirius, with an emission peak at 424 nm, the shortest emission wavelength among fluorescent proteins reported to date. The pH-insensitivity of Sirius allowed prolonged visualization of biological events in an acidic environment. Two fluorescence resonance energy transfer (FRET) pairs, Sirius-mseCFP and Sapphire-DsRed, allowed dual-FRET imaging with single-wavelength excitation, enabling detection of $Ca^{2+}$ concentration and caspase-3 activation in the same apoptotic cells.**

Among the fluorescent proteins reported to date, the variant with a Phe66 mutation in wild-type *Aequorea Victoria* GFP has the shortest emission wavelength, with a peak at 442 nm[1]. However, fluorescence quantum yield of the GFP-Phe66 variant is low ($\Phi_{Fl} = 0.013$), strictly limiting its applicability for bioimaging.

To evolve the dim GFP-Phe66 mutant into a bright fluorescent protein, we randomly mutagenized the sequence encoding four amino acids surrounding the chromophore of mseCFP-W66F, which had been made by introducing the W66F mutation into the cyan fluorescent protein variant, mseCFP (ref. 2) (**Table 1** and **Supplementary Fig. 1** online). One resulting protein containing four substitutions (T65Q, Y145G, H148S and T203V; **Supplementary Fig. 1**) was an ultramarine fluorescent protein with a 25-fold increase in fluorescence intensity (**Fig. 1a** and **Supplementary Fig. 2** online). This protein, UMFP-1, had an emission peak at 424 nm and a bimodal absorption peak at 280 and 355 nm (**Fig. 1b**). Owing to its greatly blue-shifted spectrum, UMFP-1 was spectrally compatible for multicolor imaging with CFP, YFP and RFP (**Fig. 1c** and **Supplementary Fig. 3** online). UMFP-1 could also be used in a detection channel distinct from BFP, for extended multicolor imaging by linear spectral unmixing (**Supplementary Fig. 4** online).

To improve the brightness of UMFP-1, we introduced an F46L mutation into the protein, yielding UMFP-2; this mutation promotes chromophore maturation at 37 °C (ref. 3). Then, we conducted two more rounds of random mutagenesis on the entire gene using error-prone PCR and obtained still-brighter mutants UMFP-3 (UMFP-2–Q69L) and UMFP-4 (UMFP-3–F223S) (**Supplementary Fig. 1**). The final variant, UMFP-4, which we named Sirius, had 80-fold brighter fluorescence than mseCFP-W66F and the same spectrum as UMFP-1 (**Table 1** and **Supplementary Fig. 2**). These increases in fluorescence intensity were mainly due to improvements in $\Phi_{Fl}$ (**Table 1**).

Notably, although Sirius had a smaller absorption coefficient ($\varepsilon$) and $\Phi_{Fl}$ than the BFPs, its fluorescence intensity in bacterial cells at 37 °C was about twice that of EBFP and two-thirds of EBFP2 (ref. 4) (**Supplementary Fig. 5a** online). We also observed a similar fluorescence intensity in mammalian cells (**Supplementary Fig. 5b**), suggesting that the Sirius chromophore underwent

**Table 1** | Physical and optical properties of ultramarine fluorescent proteins variants

| Protein | Color | $\lambda_{ab}$[a] (nm) | $\lambda_{em}$[b] (nm) | $\varepsilon$ ($M^{-1}cm^{-1}$) | $\Phi_{Fl}$ | pKa | $\tau_{bleach}$[c] (arc lamp) | $\tau_{bleach}$ (laser) | $\Phi_{bleach}$ ($\times10^{-6}$) | Relative fluorescence[d] *Escherichia coli* | Relative fluorescence[d] HEK293 | $K_{ox}$[e] ($\times10^{-4}$ $s^{-1}$) |
|---|---|---|---|---|---|---|---|---|---|---|---|---|
| mseCFP | Cyan | 434 | 474 | 30,000 | 0.4 | 6.4 | – | – | – | – | – | – |
| mseCFP-W66F | Ultramarine | 355 | 424 | 14,000 | 0.003 | – | – | – | – | – | – | – |
| UMFP-1 | Ultramarine | 355 | 424 | 15,000 | 0.07 | <3.0 | – | – | – | – | – | – |
| UMFP-2 | Ultramarine | 355 | 425 | 15,000 | 0.11 | <3.0 | – | – | – | – | – | – |
| UMFP-3 | Ultramarine | 355 | 424 | 13,000 | 0.16 | <3.0 | – | – | – | – | – | – |
| UMFP-4 (Sirius) | Ultramarine | 355 | 424 | 15,000 | 0.24 | <3.0 | 62 | 7.3 | 9.79 | 2.2 | 1 | 5.6 |
| EBFP2 | Blue | 380 | 447 | 34,000 | 0.54 | 5.7 | 13 | 9.9 | 5.12 | 2.8 | 1.8 | 4.4 |
| EBFP | Blue | 380 | 448 | 32,000 | 0.25 | 6.3 | 1 | 1 | 113 | 1 | 1 | 4.7 |

[a]Absorption wavelength peak. [b]Emission wavelength peak. [c]Time needed to bleach 1/e of maximum fluorescence intensity in HeLa cells ($n = 3$) relative to EBFP. [d]Fluorescence intensity relative to that of EBFP in *E. coli* and HEK293 at 37 °C. The amount of protein in *E. coli* was estimated by measuring absorption at 600 nm. The amount of protein in HEK293 was determined by western blotting with antibody to GFP. [e]Time constant of oxidation. –, not determined.

[1]Laboratory for Nanosystems Physiology, Research Institute for Electronic Science, Hokkaido University, Sapporo, Hokkaido, Japan. [2]Supportive Center for Brain Research, National Institute for Physiological Science, Okazaki, Aichi, Japan. [3]Nikon Imaging Center, Research Institute for Electronic Science, Hokkaido University, Sapporo, Hokkaido, Japan. Correspondence should be addressed to T. Nagai (tnagai@es.hokudai.ac.jp).

RECEIVED 2 JANUARY; ACCEPTED 12 FEBRUARY; PUBLISHED ONLINE 6 APRIL 2009; DOI:10.1038/NMETH.1317

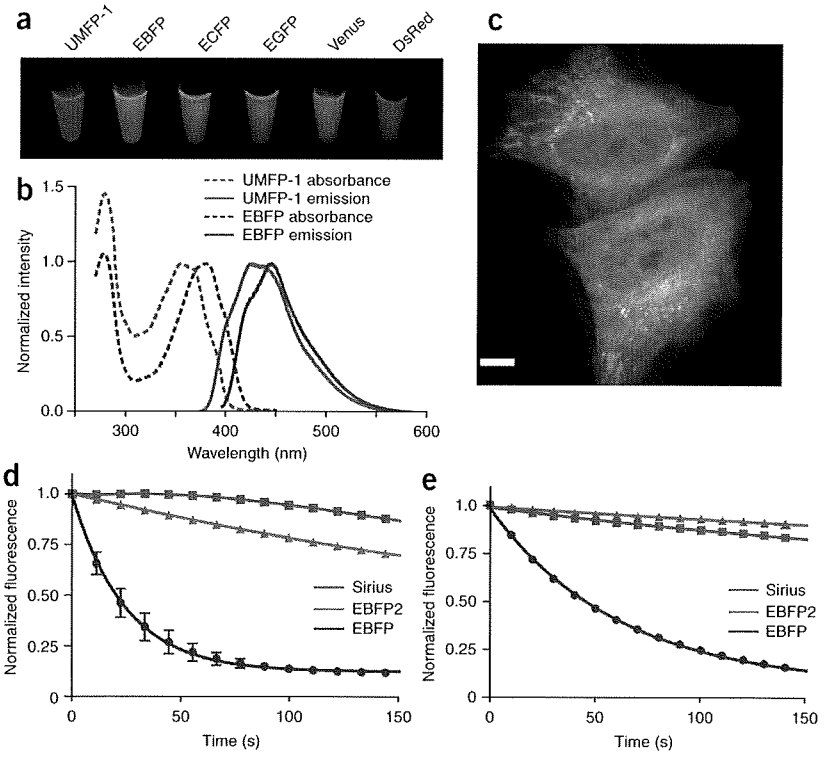


**Figure 1** | Characterization of UMFP variants. (**a**) Fluorescence of purified UMFP-1 and conventional fluorescent proteins, with 365-nm excitation. (**b**) Absorption and emission spectra of UMFP-1 and EBFP. (**c**) Multicolor imaging of HeLa cells with UMFP-1–labeled nuclei (red), mseCFP–labeled endoplasmic reticulum (cyan), Venus–labeled mitochondria (yellow) and mCherry–labeled microtubules (magenta). Scale bar, 10 μm. (**d**,**e**) Photobleaching curves of Sirius, EBFP2 and EBFP in HeLa cells, excited by a mercury arc lamp through a 352-nm–388-nm excitation filter (**d**) and using a 375-nm diode laser (**e**). All curves were normalized to the fluorescence intensity before photobleaching. Error bars, s.d. ($n = 3$).

efficient post-translational maturation in the intracellular environment at 37 °C. Concordantly, the rate of Sirius's chromophore oxidation, which is the rate-limiting step of chromophore formation, was larger than that for either EBFP or EBFP2 (**Table 1** and **Supplementary Fig. 5c**).

Because one of the mutated amino acids (F223S) in Sirius faced outside of the protein, it was possible that Sirius had different oligomerization properties than mseCFP. However, the fluorescence signal of Sirius expressed in HeLa cells was evenly distributed in the cytoplasm and nucleus without any visible aggregates or nonspecific localization (**Supplementary Fig. 6a** online), suggesting that it is a monomer, although this would need to be confirmed by additional analysis. Sirius fusions did not perturb the localization of several fusion partners (**Supplementary Fig. 6b–i**); an exception was the fusion of Sirius with α-tubulin, which localized to microtubules but was also found in the cytoplasm (data not shown). Optimization of amino acid linker length between Sirius and α-tubulin may improve the localization.

When compared with EBFP and EBFP2 in HeLa cells, the photobleaching kinetics of Sirius using a mercury arc lamp was 62 times and 5 times slower than that of EBFP and EBFP2, respectively (**Fig. 1d** and **Table 1**). Furthermore, although the bleaching curves of EBFPs showed single exponential decay, those of Sirius exhibited two components: a flat, stable component followed by exponential decay, suggesting a complicated bleaching process (**Fig. 1d**). However, we observed simple exponential decay for both Sirius and EBFP2 when they were bleached by an intense 375 nm laser. (**Fig. 1e** and **Table 1**). We also calculated the quantum yield for photobleaching ($\Phi_{bleach}$) that does not depend on the absorption coefficient ($\varepsilon$) of each fluorescent protein (**Table 1** and **Supplementary Methods** online). $\Phi_{bleach}$ of Sirius ($9.79 \times 10^{-6}$) was much smaller than that of EBFP ($1.13 \times 10^{-4}$) and comparable to that of EBFP2 ($5.12 \times 10^{-6}$).

The most noteworthy feature of Sirius is its fluorescence stability in a wide range of proton concentrations (pH 3–9) (**Fig. 2a**). Presumably, this is due to the Phe66 mutation of the chromophore, as the resulting benzyl, unlike phenol, has no ionizable group. This pH-insensitivity of Sirius may make it highly suitable for fluorescence imaging in acidic environments, such as in phagosomes. We observed phagocytosis of fluorescent protein–expressing bacteria by *Dictyostelium discoidium*. We used two-photon excitation by a 780-nm pulse laser to minimize photodamage induced by wide-field UV-light excitation of the highly photosensitive *Dictyostelium*

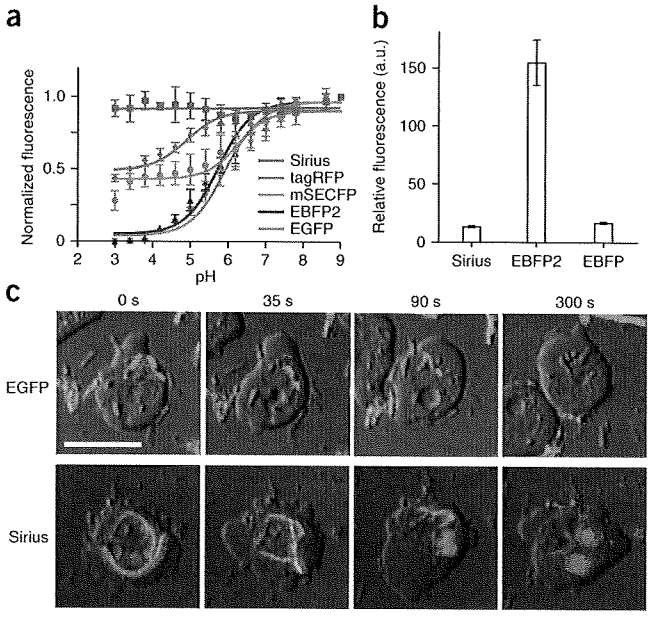


**Figure 2** | pH-sensitivity of Sirius. (**a**) pH dependence of the fluorescence emission of the indicated purified proteins. Data are mean ± s.d. ($n = 3$). (**b**) Mean fluorescence intensity of the indicated proteins expressed in HeLa cells ($n = 30$), under two-photon excitation at 780 nm. Error bars, s.e.m. (**c**) Differential interference contrast images merged with corresponding fluorescence images, monitoring phagocytosis of fluorescent protein–expressing bacteria by *Dictyostelium discoidium* at the indicated times. Scale bar, 5 μm.

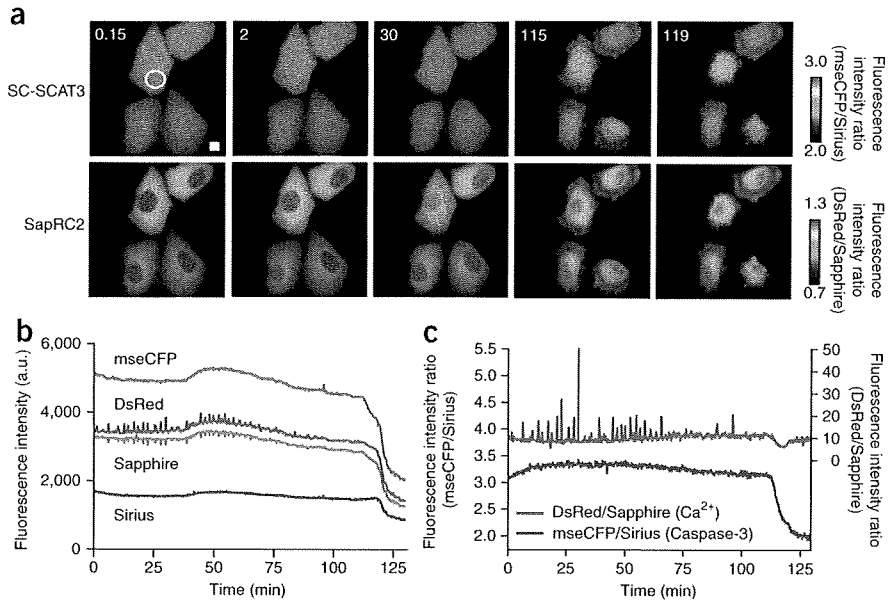


**Figure 3** | Dual functional imaging with two FRET pairs. (**a**) Pseudocolored ratio images of representative HeLa cells expressing SC-SCAT3 (top) and SapRC2 (bottom), at the indicated times (in minutes) after treatment with TNF-alpha. The color bars represent the cyan-to-ultramarine fluorescence intensity ratio (mseCFP/Sirius; top) or red-to-green intensity ratio (DsRed/Sapphire; bottom). Scale bar, 10 μm. (**b**) Time course of the fluorescence intensity after four-color spectral linear unmixing in the region circled in **a** (a.u., arbitrary units). (**c**) Fluorescence intensity ratio of mseCFP/Sirius and DsRed/Sapphire after four-color spectral unmixing in the region circled in **a**.

cells. Although the excitation of Sirius at 780 nm was not effective when compared with that of EBFP2 (**Fig. 2b**), it was sufficient to identify Sirius-expressing specimens. Using EGFP-expressing bacteria, the fluorescence signal disappeared before the bacteria were completely digested in phagosomes (**Fig. 2c** and **Supplementary Video 1** online). In contrast, using Sirius-expressing bacteria, we could visualize the entire process of phagocytosis (**Fig. 2c** and **Supplementary Video 1**).

Sirius is potentially an ideal donor to pair with mseCFP for fluorescence resonance energy transfer (FRET), since the emission spectrum of Sirius overlaps substantially with the absorption spectrum of mseCFP (**Supplementary Fig. 7a** online). However, the spectral overlap ($J = 0.71 \times 10^{-13}\ M^{-1}\ cm^3$) is smaller than in some other FRET pairs, such as CFP-YFP ($J = 1.89 \times 10^{-13}\ M^{-1}\ cm^3$), owing to the fourth power wavelength dependency of $J$. Also, when assuming $\kappa^2 = 2/3$, the Förster distance ($R_0$) of Sirius-mseCFP pair ($R_0 = 3.7$ nm) is smaller than that of CFP-YFP ($R_0 = 4.7$ nm) (**Supplementary Table 1** online) because of the lower $\Phi_{FI}$ of Sirius. Despite these drawbacks, the Sirius-mseCFP fusion protein (joined by a Leu-Glu peptide linker) showed a moderate sensitized emission from mseCFP, with 43% FRET efficiency (**Supplementary Fig. 7b,c** and **Supplementary Note 1** online). Encouraged by this result, we constructed an indicator for caspase-3 activation[5] by fusing the caspase-3 substrate Asp-Glu-Val-Asp between Sirius and mseCFP, yielding SC-SCAT3. We then monitored the change in FRET signal of SC-SCAT3 in apoptotic HeLa cells. As shown previously[6], we visualized caspase-3 activation first in the cytoplasm and then in the nucleus, which was followed by cell shrinking.

Recently, multiple-FRET imaging by using two independently excitable FRET pairs has been reported[7]. Because the FRET donors have distinct excitation profiles, there was only slight cross-excitation, allowing an accurate ratiometric measurement of the two FRET indicators. We expanded the dual FRET imaging arsenal with a different strategy that makes use of two FRET pairs, Sirius-mseCFP and Sapphire-DsRed (**Supplementary Fig. 7d**), both of which can be excited with a single wavelength (380 nm; or 720 nm by two-photon excitation) (**Supplementary Fig. 7e**). In combination with linear spectral unmixing[8], this allows single-excitation quadruple-emission measurements, even if both FRET pairs are present at the same intracellular location. To verify this method, we expressed SC-SCAT3 and SapRC2, a $Ca^{2+}$-indicator based on Sapphire and DsRed[9], in HeLa cells. Upon apoptosis induction with TNF-alpha, we observed $Ca^{2+}$ oscillation within the first 90 min, and then it ceased[10]; in contrast, we observed caspase-3 activation at around 120 min after induction (**Fig. 3, Supplementary Video 2** and **Supplementary Note 2** online). Such dual FRET imaging should allow a variety of experiments to elucidate the dynamic relationships among multiple biological phenomena in a single cell.

**Accession codes.** GenBank, EMBL Nucleotide Sequence Database and DNA Databank of Japan: AB444952 (nucleotide sequence encoding Sirius).

*Note: Supplementary information is available on the Nature Methods website.*

**ACKNOWLEDGMENTS**

We thank R.E. Campbell (University of Alberta) and A. Miyawaki (RIKEN) for providing the cDNA encoding EBFP2 and SapRC2, respectively. This work was partly supported by grants from Scientific Research on Advanced Medical Technology of the Ministry of Labor, Health and Welfare of Japan and the Japanese Ministry of Education, Science and Technology.

**AUTHOR CONTRIBUTIONS**

W.T. performed experiments and data analysis; T.M. and I.K. contributed to gene construction; T.T., To.N. and K.S. set up microscopy systems; K.H. contributed to imaging of phagocytosis; Ta.N. contributed to the conceptual development, experimental design, data analysis and manuscript preparation.

**Published online at http://www.nature.com/naturemethods/**
**Reprints and permissions information is available online at http://npg.nature.com/reprintsandpermissions/**

1. Cubitt, A.B. *et al. Trends Biochem. Sci.* **20**, 448–455 (1995).
2. Matsuda, T., Miyawaki, A. & Nagai, T. *Nat. Methods.* **5**, 339–345 (2008).
3. Nagai, T. *et al. Nat. Biotechnol.* **20**, 87–90 (2002).
4. Ai, H.W., Shaner, N.C., Cheng, Z., Tsien, R.Y. & Campbell, R.E. *Biochemistry* **46**, 5904–5910 (2007).
5. Xu, X. *et al. Nucleic Acids Res.* **26**, 2034–2035 (1998).
6. Takemoto, K., Nagai, T., Miyawaki, A. & Miura, M. *Cell Biol.* **160**, 235–243 (2003).
7. Ai, H.W., Hazelwood, K.L., Davidson, M.W. & Campbell, R.E. *Nat. Methods.* **5**, 401–403 (2008).
8. Zimmermann, T., Rietdorf, J. & Pepperkok, R. *FEBS* **546**, 87–92 (2003).
9. Mizuno, H., Sawano, A., Eli, P., Hama, H. & Miyawaki, A. *Biochemistry* **40**, 2502–2510 (2001).
10. Pu, Y., Luo, K.Q. & Chang, D.C.A. *Biochem. Biophys. Res. Commun.* **299**, 762–769 (2002).

nature | methods

# An ultramarine fluorescent protein with increased photostability and pH insensitivity

Wataru Tomosugi, Tomoki Matsuda, Tomomi Tani, Tomomi Nemoto, Ippei Kotera, Kenta Saito, Kazuki Horikawa & Takeharu Nagai

Supplementary figures and text:

| Supplementary File | Title |
|---|---|
| **Supplementary Figure 1** | Sequence alignment of UMFP and GFP variants. |
| **Supplementary Figure 2** | Comparative characterization of the absorption and fluorescence properties of UMFP variants. |
| **Supplementary Figure 3** | Multi color imaging of HeLa cells stained by four color variants of fluorescent protein. |
| **Supplementary Figure 4** | Dual color imaging of UMFP-mito and EBFP-H2B in HeLa cells by linear spectral unmixing. |
| **Supplementary Figure 5** | Fluorescence emission intensity of Sirius, EBFP, and EBFP2 at 37 oC. |
| **Supplementary Figure 6** | HeLa cells expressing Sirius or a Sirius fusion protein. |
| **Supplementary Figure 7** | Dual FRET imaging by single-excitation-quadruple-emission measurement mode. |
| **Supplementary Table 1** | Förster radius (nm) of the fluorescent protein pairs. |
| **Supplementary Note 1** | Photobleaching of CFP. |
| **Supplementary Note 2** | Linear unmixing of dual FRET measurement. |
| **Supplementary Methods** | |

*Note: Supplementary Videos 1 and 2 are available on the Nature Methods website.*

Nature Methods: doi:10.1038/nmeth.1317

**Supplementary Figure 1.** Sequence alignment of UMFP and GFP variants.

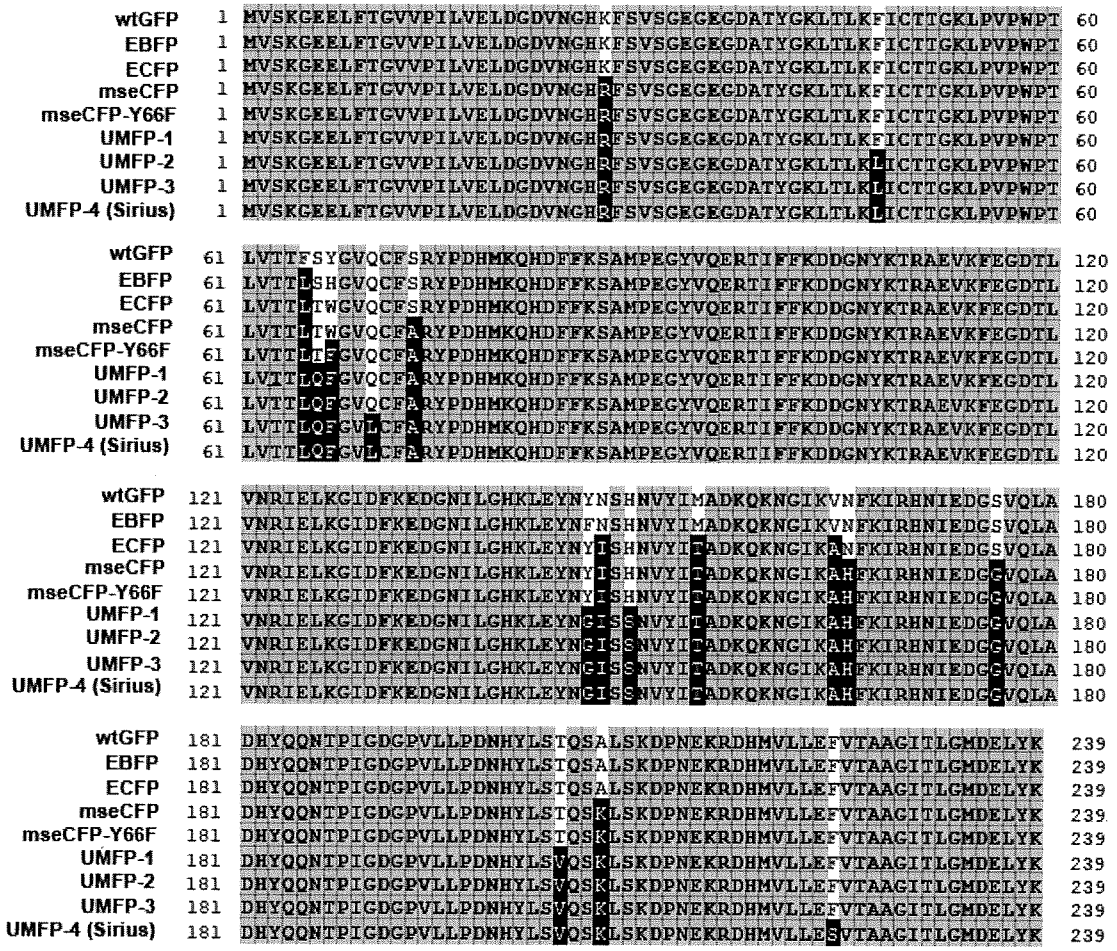


Sequences show the alignment of *Aequorea victoria* wild-type GFP, EBFP, ECFP, mseCFP, mseCFP-Y66F, UMFP-1, UMFP-2, UMFP-3 and UMFP-4(Sirius). The texts on gray background show the retained amino acids for mutagenesis. Mutations related to UMFP-4(Sirius) are indicated as white text on a black background.

**Supplementary Figure 2.** Comparative characterization of the absorption and fluorescence properties of UMFP variants.

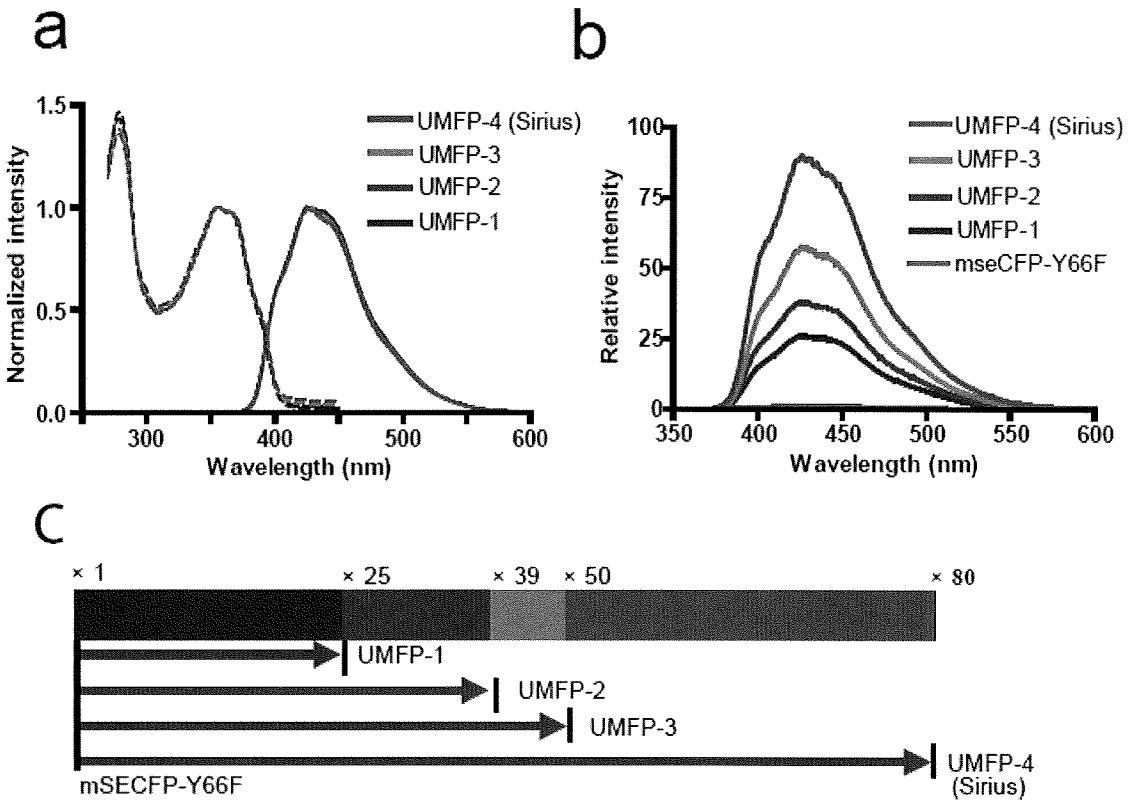


(**a**) Absorption (dotted lines) and emission spectra (solid lines) of UMFP variants. (**b**) Fluorescence emission spectra of purified UMFP variants: mseCFP-Y66F, UMFP-1, UMFP-2, UMFP-3, and UMFP-4. (**c**) Brightness of fluorescence by calculation of extinction coefficient and quantum yield of UMFP variants. Brightness was normalized to the fluorescence of mseCFP-W66F.

**Supplementary Figure 3.** Multi color imaging of HeLa cells stained by four color variants of fluorescent protein.

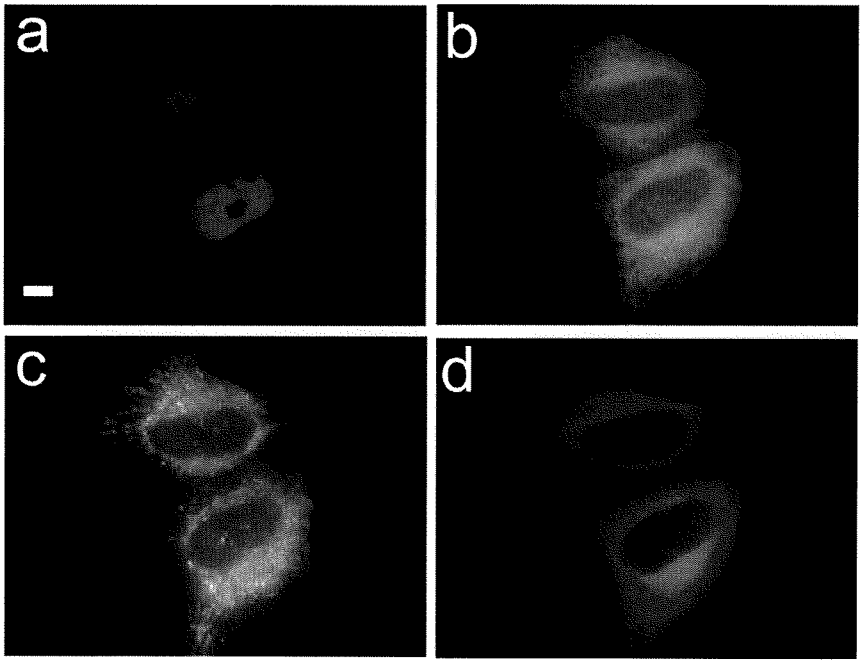


(a) UMFP-1–labeled nuclei, (b) mseCFP–labeled endoplasmic reticulum, (c) Venus–labeled mitochondria, (d) mCherry–labeled microtubles, Scale bar, 10 μm

**Supplementary Figure 4.** Dual color imaging of UMFP-mito and EBFP-H2B in HeLa cells by linear spectral unmixing.

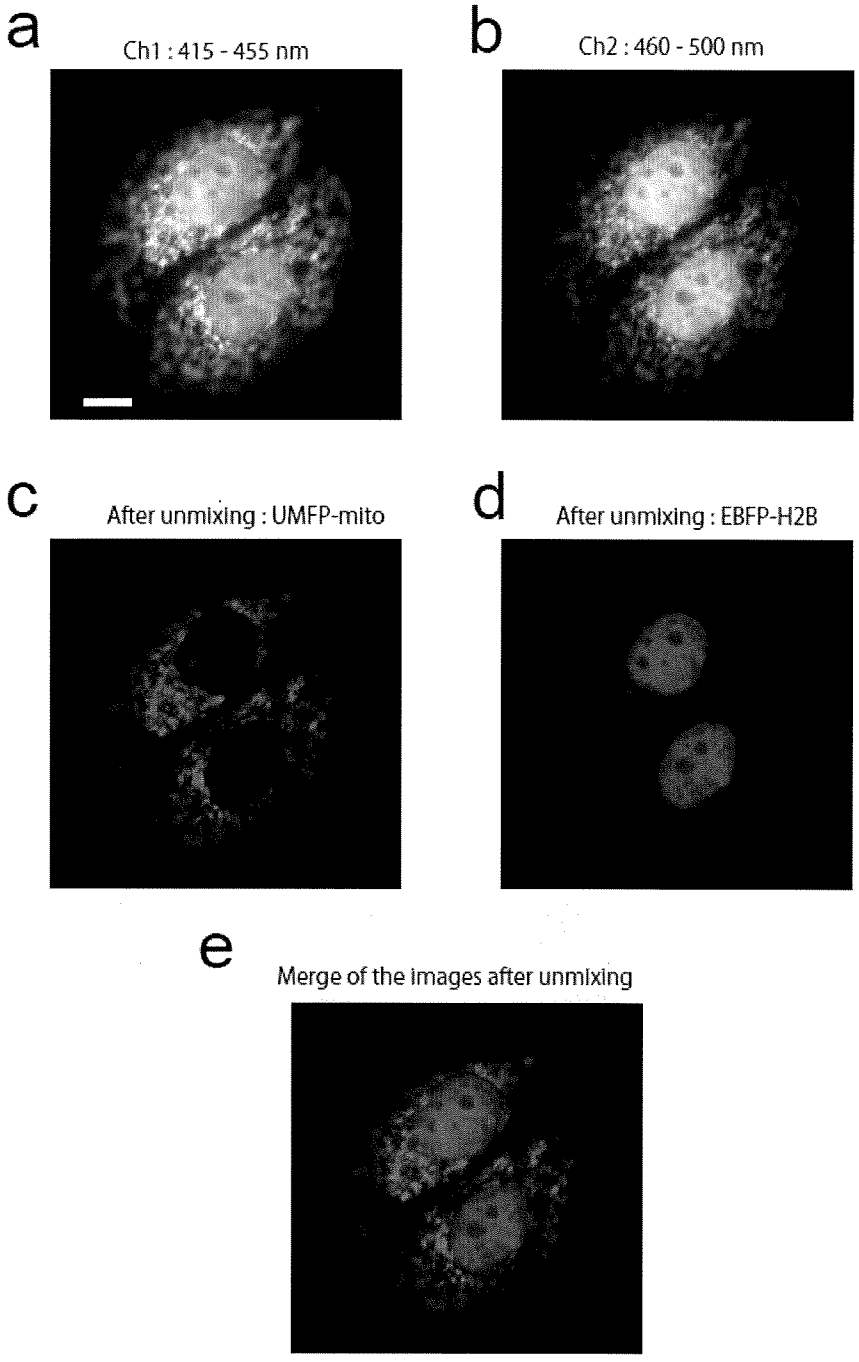


(**a, b**) Fluorescence images taken through detection channel 1 (Ch1: 415 - 455 nm) (a) and detection channel 2 (Ch2: 459 – 499 nm) (b). (**c, d**) Fluorescence images of UMFP-mito (c: green) and EBFP-H2B (d: magenta) after linear spectral unmixing. (**e**) The image created by merging the images in c and d. Scale bar, 10 μm.

**Supplementary Figure 5.** Fluorescence emission intensity of Sirius, EBFP, and EBFP2 at 37 °C.

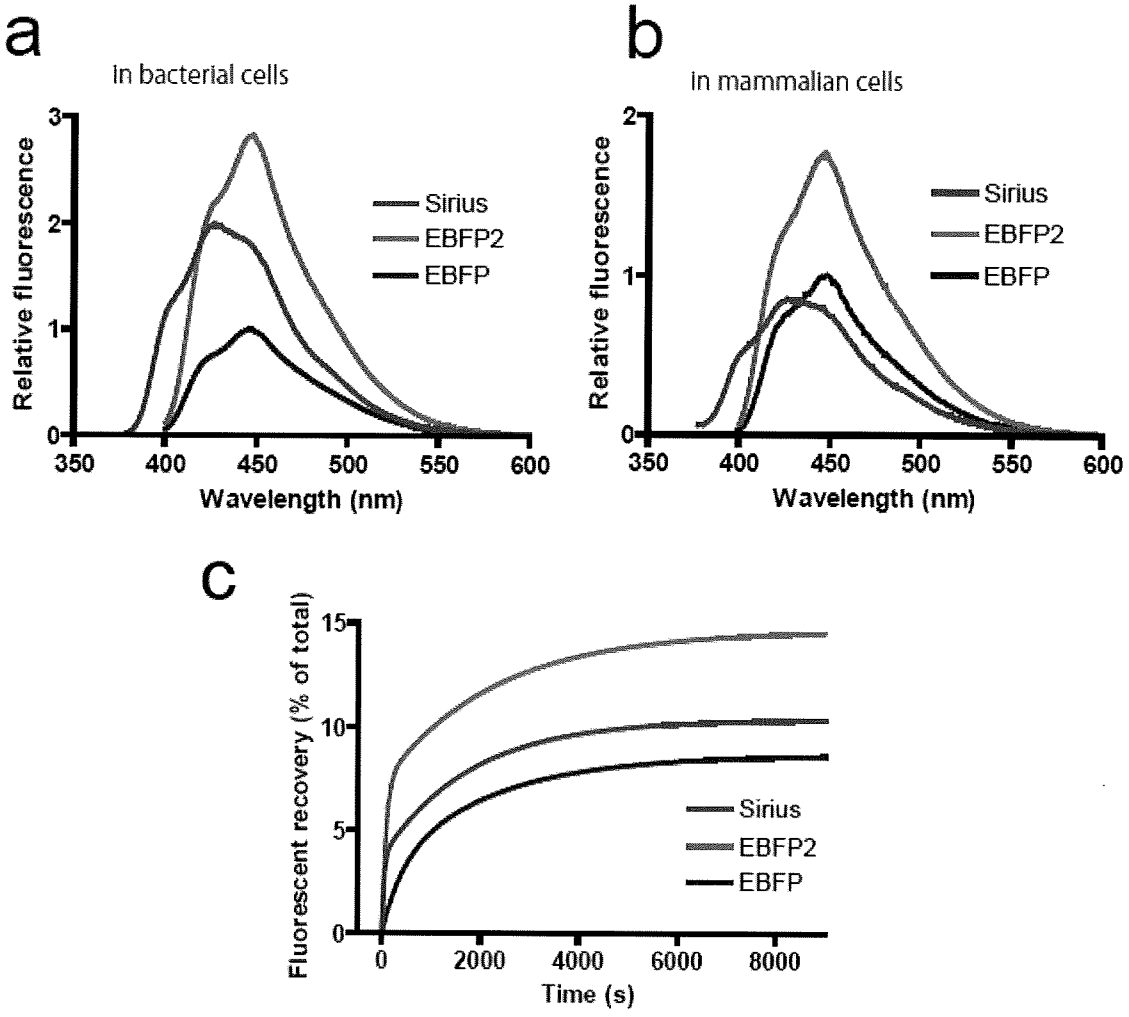


Relative emission spectra in *E. coli* (**a**) and HEK293 cells (**b**) cultured at 37 °C. Sirius was excited at 355 nm. EBFP2 and EBFP were excited at 380 nm. (**c**) Fluorescence acquisition curve of Sirius (red), EBFP2 (cyan), and EBFP (blue) in solution at 37 °C.

**Supplementary Figure 6.** HeLa cells expressing Sirius or a Sirius fusion protein.

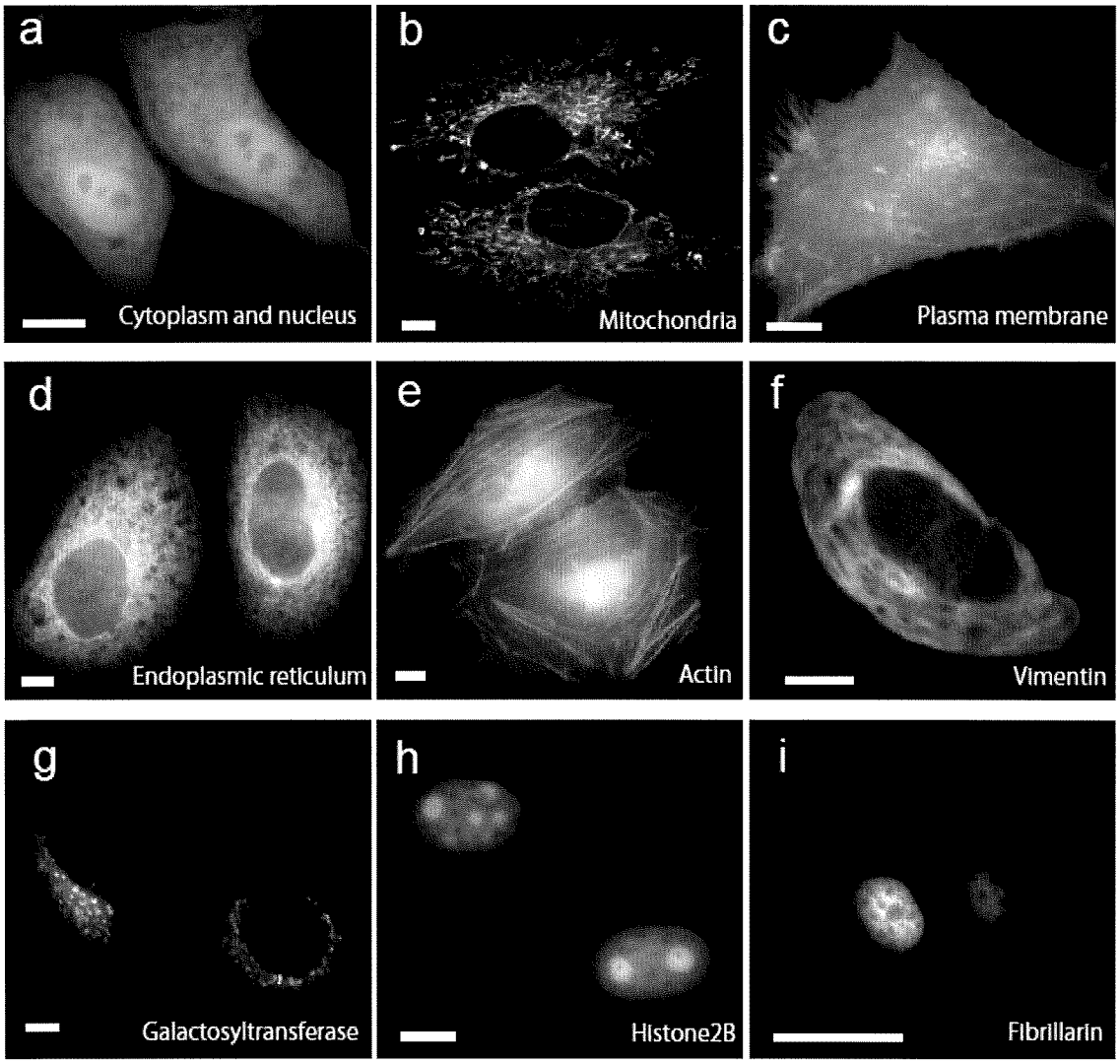


(**a**) Sirius, (**b**) Sirius-mito, (**c**) Sirius–pm, (**d**) Sirius-er, (**e**) Sirius-actin, (**f**) Sirius-vimentin, (**g**) Sirius-Golgi, (**h**) Sirius-H2B, and (**i**) Sirius-fibrillarin Scale bars, 10μm.

**Supplementary Figure 7**. Dual FRET imaging by single-excitation-quadruple-emission measurement mode.

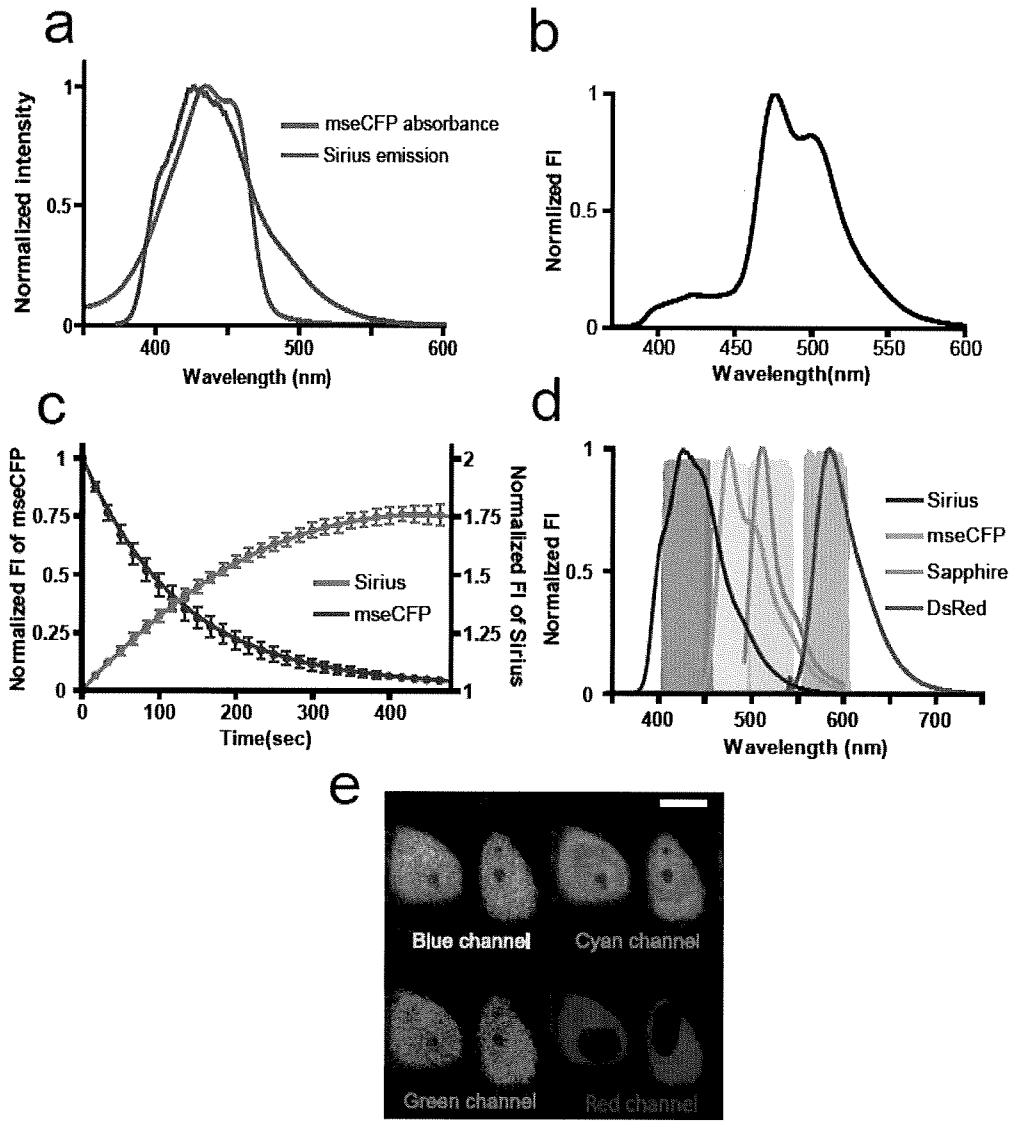


(**a**) Spectral overlap between Sirius emission (red) and mseCFP absorption (cyan). (**b**) The emission spectrum of purified Sirius-mseCFP fusion protein by excitation at 360 nm. (**c**) Time course of changing in fluorescence intensity of Sirius and mseCFP in Sirius-mseCFP fusion protein during acceptor photobleaching. Error bars are s.d (n=3). (**d**) The emission spectrum of Sirius, mseCFP, Sapphire, and DsRed. Transparent colors represent the emission filters used to acquire each fluorescent protein signal for the dual FRET imaging. (**e**) Dual-FRET imaging of SC-SCAT3 and SapRC2 in HeLa cells by two-photon excitation at 720nm. Scale bars, 30μm.

**Supplementary Table 1.** Förster radius (nm) of the fluorescent protein pairs.

| | | Donor | | | | | |
|---|---|---|---|---|---|---|---|
| | | Sirius | EBFP | ECFP | EGFP | EYFP | DsRed1 |
| **Acceptor** | Sirius | — | — | — | — | — | — |
| | EBFP | 2.8 | — | — | — | — | — |
| | ECFP | 3.7 | 3.9 | — | — | — | — |
| | EGFP | 4.0 | 4.2 | 5.2 | — | — | — |
| | EYFP | 3.7 | 3.9 | 4.7 | 5.6 | — | — |
| | DsRed1 | 4.1 | 4.3 | 5.2 | 5.9 | 6.1 | — |

**Supplementary Note 1**

Photobleaching of CFP. We obtained FRET efficiency in Sirius-mseCFP FRET pair by measuring dequenching of donor (Sirius) emission after acceptor (mseCFP) photobleaching. In the experiment, the fluorescence intensity of Sirius was increased 1.75 fold (**Supplementary Fig. 6c**), from which we calculated about 43% FRET efficiency. However, the increase in Sirius fluorescence might contain the signal from photoconverted mseCFP upon photobleaching. To exclude the possibility of mseCFP photoconversion to a more blue-shifted spectrum especially overlapping with emission spectrum of Sirius, we performed a control experiment to show no photoconversion of mseCFP upon photobleaching. As shown in **Fig. A**, we did not see any detectable photoconversion of mseCFP. Therefore, we concluded that the 43% FRET efficiency in Sirius-mseCFP obtained from the acceptor mseCFP bleaching experiment was appropriate.

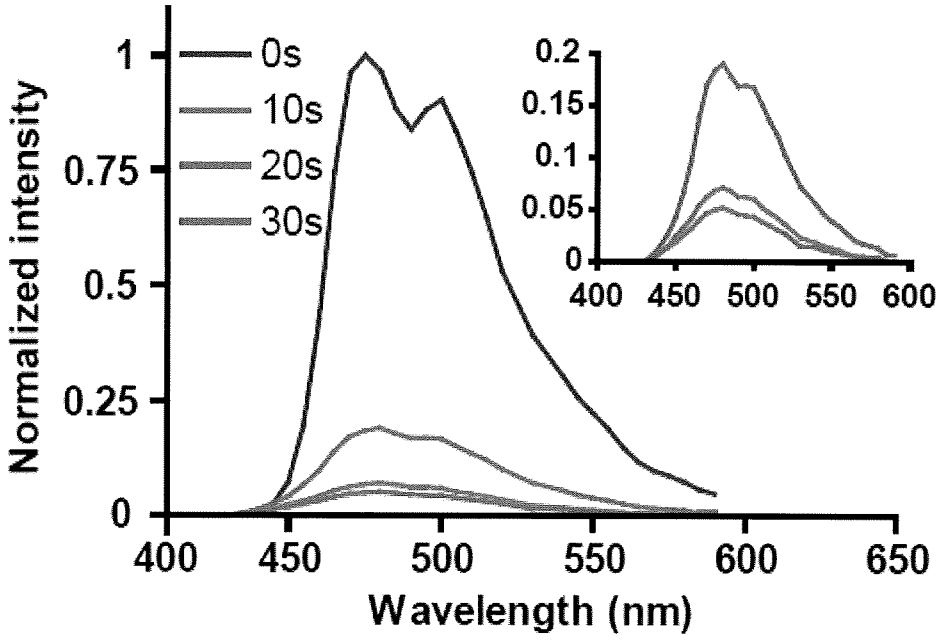


**Figure A. Emission spectra of mseCFP during photobleaching in a HeLa cell.** mseCFP expressing in living HeLa cells were photobleached by intense excitation with 405 nm laser diode under an inverted microscope. Times indicated in the panel show the total time of photobleaching. An inset graph shows the data with expanded ordinate.

**Supplementary Note 2**

Linear unmixing of dual FRET measurement. Although the two FRET pairs, Sirius-mseCFP and Sapphire-DsRed have an advantage such that they can use common excitation wavelength since both Sirius and Sapphire can be excited at 380 nm. However, we have to carefully consider bleed through signals of Sirius and mseCFP into channels for Sapphire and DsRed detection (**Fig. Ba**) because the bleed through signals greatly influence to DsRed/Sapphire emission ratio value (**Fig. Bb**), especially when mseCFP intensity signal is much larger than that of Sapphire (**Fig. Bc**). In this case, spectral unmixing technique can be used to remove the bleed through signal (**Fig. Bd**). We also confirmed this by co-expressed SC-SCAT3 and SapRC2 in HeLa cells (compare **Fig. Be, Fig. Bf** and **Fig. 3c**) Meanwhile, we might be able to minimize the bleed through effect by choosing cells with larger Sapphire signal than that of mseCFP because the relatively small mseCFP signal does not significantly influence the value of DsRed/Sapphire emission ratio (**Fig. Bg,h**).

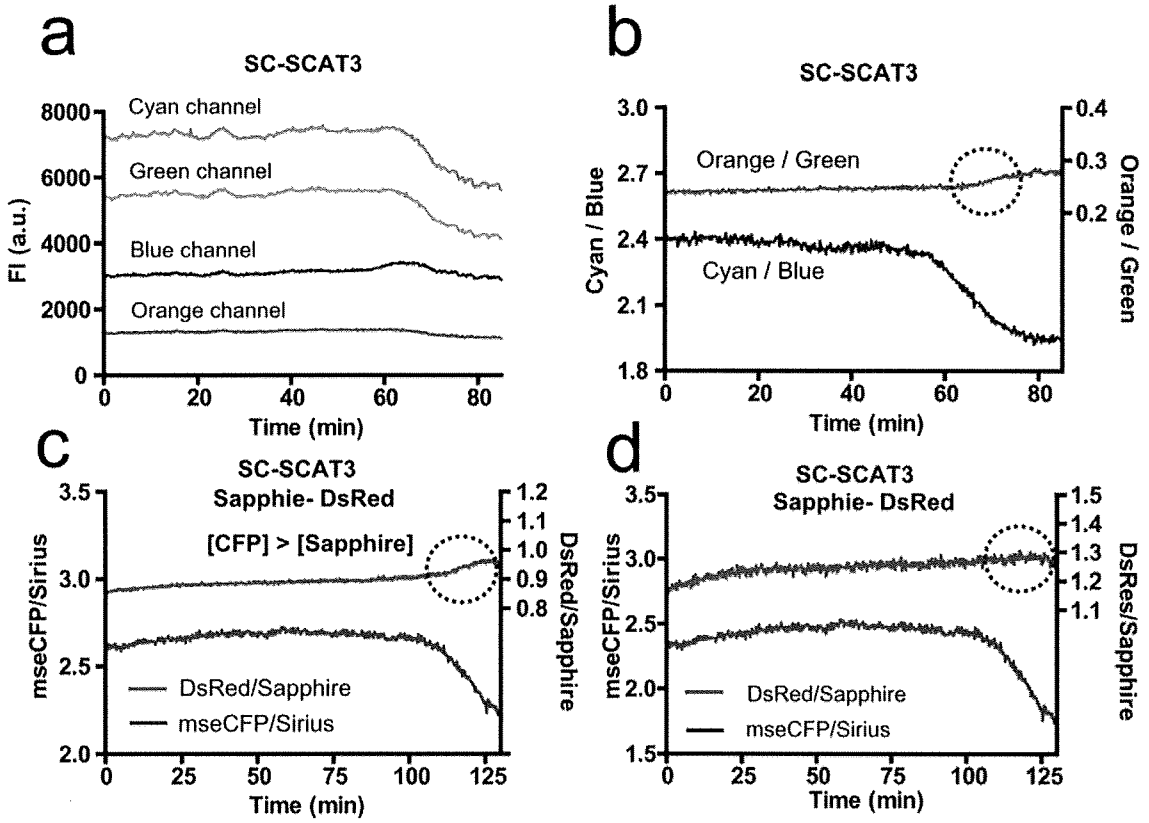

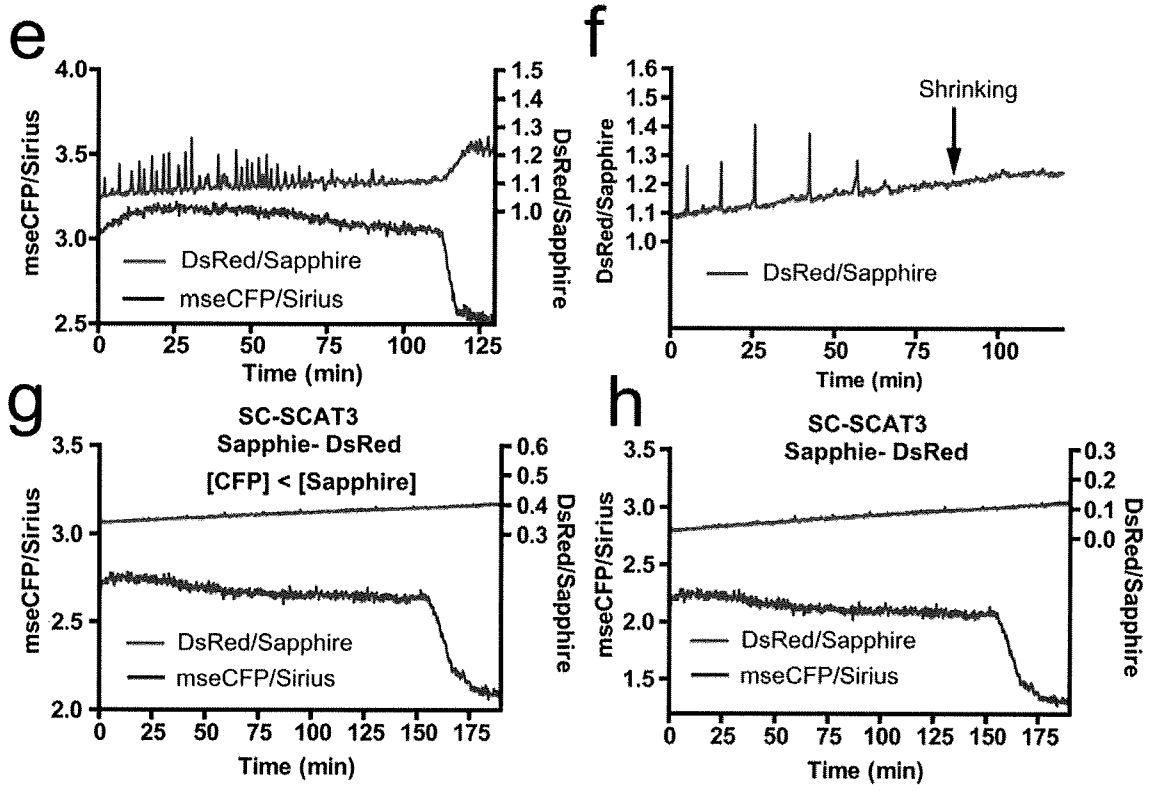


**Figure B.** The effect of bleed through on intensity ratio. (**a,b**) Time course of the fluorescence intensity (a) and intensity ratio (b) of HeLa cells expressing only SC-SCAT3 measuring through the emission filters for blue, cyan, green and orange acquisition. a.u, arbitrary units. Dotted circles indicate the change of ratio derived from bleed through. (**c, d**) Time course of intensity ratio in HeLa cells expressing both SC-SCAT3 and Sapphire-DsRed (joined by a LE amino acid) without (c) and with (d) four colors unmixing. Shown is the result obtained from the cells in which fluorescence intensity of mseCFP is larger than that of Sapphire. (**e**) Time course of the intensity ratio of both mseCFP/Sirius (blue line) and DsRed/Sapphire (red line) before four colors unmixing in the regions of interest shown in Fig.3a. **(f)** Time course of the intensity ratio of HeLa cells expressing only SapRC2 measuring after TNF-alpha treatment. The arrow indicates the start of cell shrinking. (**g, h**) Time course of intensity ratio in HeLa cells expressing both SC-SCAT3 and Sapphire-DsRed (joined by a LE amino acid) without (g) and with (h) four colors unmixing. Shown is the result obtained from the cells in which fluorescence intensity of mseCFP is smaller (g, h) than that of Sapphire.

## Supplementary Methods

**Gene construction.** The Sirius-mseCFP fusion protein was made by coupling C-terminally truncated Sirius and N-terminally truncated mseCFP, as shown previously[12]. The cDNA of C-terminally truncated Sirius was amplified by PCR using a sense primer, 5'-GCGGATCCGATGGTGAGCAAGGGCGAGGAG-3,' containing a *BamH*I site, and an antisense primer, 5'-TTATCTCGAGGGCGGCGGTCACGAACTCCA-3', containing an *Xho*I site before the Ala227 codon of Sirius. The cDNA of N-terminally truncated mseCFP was amplified by PCR using a sense primer, 5'-GCCTCGAGGAGGAGCTGTTCACCGGG-3', containing an *Xho*I site before the codon for Glu5 and an antisense primer, 5'-GCGAATTCTTACTTGTACAGCTCGTCCATGC-3', containing a termination codon followed by an *Eco*RI site. The restriction products were cloned into the *Bam*HI and *Eco*RI sites of $pRSET_B$ (Invitrogen) for bacterial expression. For mammalian expression, the *Bam*HI-*Eco*RI fragment of Sirius-mseCFP was subcloned into pcDNA3 (Invitrogen). UMFP1-H2B and EBFP-H2B in mammalian expression vectors were constructed by replacing the Phamret in Phamret-H2B-pcDNA3[2] with UMFP-1 and EBFP, respectively. mCherry-Tub and Venus-mito in mammalian expression vectors were constructed by replacing EYFP in pEYFP-Tub (Clontech) with mCherry[13], and by fusing the 12 N-terminal amino acids of the cytochrome c oxidase subunit IV presequence to the N terminus of Venus[3], respectively. mseCFP-er was generated by extending mseCFP at the N terminus with the signal peptide from calreticulin and at the C terminus with an ER retention signal[14]. For the imaging of Sirius fusion constructs,

Sirius-Mito, Sirius-Golgi, Sirius-H2B, Sirius-fibrillarin and Sirius-Tub in mammalian expression vectors were constructed by replacing the Phamret in Phamret-mit-pcDNA3[2], Phamret-peroxisome-pcDNA3[2], Phamret-Golgi-pcDNA3[2], Phamret-H2B-pcDNA3[2], Phamret-fibrillarin-pcDNA3[2], and the EYFP in pEYFP-Tub (Clontech) with Sirius. Sirius-pm was constructed by adding the myristoylation and palmitoylation sequence from lyn kinase (MGCIKSKRKDNLNDDGVDMKT) to N terminus[15]. Sirius-er was constructed such as making of mseCFP-er. β-actin and Vimentin were inserted into C-terminal and N-terminal of Sirius in pcDNA3 respectively. β-actin and vimentin have 20 (GGSGGSGGSGGSGGQFQIST) amino acid residues and 18 (GDPPVATGGSGGSGGSGG) amino acid residues as linker peptide. UC-SCAT3-pcDNA3.1(-) was constructed by replacing Venus in SCAT3-pcDNA3.1(-)[5] with Sirius. The SapRC2-pcDNA3[8] was kindly provided by Dr. Atsushi Miyawaki. The cDNA sequences for all the fluorescent protein variants were confirmed by dye terminator cycle sequencing using Big Dye (Applied Biosystems).

**Screening.** After transformation of *Escherichia coli* [JM109(DE3)] with the mutagenized DNAs, the bacteria were grown up on agar plates (10 cm in diameter) at 37°C for 16 hrs to allow the fluorescence to develop. Colonies with brighter fluorescence were picked under a MVX10 Macro View microscope with a U-MWU2 filter cube (BP330-385 excitation filter, DM400 dichroic mirror, and BA420 emission filter), and cultured overnight in 1.5 mL of LB medium containing 0.1 mg/mL carbenicillin.

**Spectroscopy.** Absorption spectra of the purified fluorescent proteins were measured on

a V-630 BIO spectrophotometer (Jasco). The protein concentrations used to calculate molar extinction coefficients were determined by the Bradford method (Protein assay kit, Bio-Rad). The fluorescent excitation and emission spectra were measured on an F-2500 fluorescence spectrophotometer (Hitachi). Fluorescence quantum yields were measured using a Hamamatsu Photonics C9920-01, an absolute photoluminescence quantum-yield measurement device.

**Measurement of fluorescence intensity at 37 °C.** *E. Coli* were transformed with Sirius-pRSET$_B$, EBFP2-pRSET$_B$ and EBFP-pRSET$_B$. After 16h culture on the LB plate at 37 °C, colonies were picked up and transfer into 2ml LB solution. After 12h culture in LB solution at 37°C, cultures were centrifuged and the pellet were suspended by PBS buffer. The bacteria suspension were diluted to $OD_{600}$ = 0.2 . The diluted solution was used for measuring the emission spectra. Measurements were done on three independent colonies. Transfection and culture of HEK293 cells were performed by FreeStyle™ 293 Expression System (invitrogen). Namely, approximately 30 μg Sirius-pcDNA3, EBFP2-pcDNA3 and EBFP-pcDNA3 were transfected into FreeStyle™ 293-F cells with concentration of 1 x $10^6$ cells/ml. After 24h culture in the medium at 37 °C, cultures were centrifuged and the pellet were suspended by PBS buffer sufficiently. The cells suspension was used in order to measure the emission spectra. For standardization of fluorescent protein amount, western blotting was carried out. Anti-GFP Poluclonal Antibody (MBL) and anti-rabbit IgG HRP (Promega) were used for primary and secondary antibody respectively. In order to detect the chemi-luminescence of HRP, SurperSignal West Dura Extended Duration Substrate Antibodies (PIERCE) was used. Purified EGFP was used as a standard of the intensity of the band. The independent

transfection was done two times.

**Measurement of protein maturation kinetics.** The oxidation kinetics of the chromophore was assessed as described[16]. Briefly, fluorescent proteins were denatured and rehydrated by incubation for 5 min at 95 °C in buffer containing 8 M urea, 1 mM DTT, and 5 mM sodium dithionite. Renaturation was initiated by 100-fold dilution in buffer containing 50 mM Tris-HCl pH 7.5, 35 mM KCl, 2 mM $MgCl_2$, 1 mM DTT at 37 °C. An equal amount of native protein was used for the normalization of fluorescence recovery.

**pH titration.** Fluorescent proteins were diluted to 2 μM in a series of 50 mM titration buffers. Glycine-HCl (pH 3.0 and 3.4), NaOAc (pH 3.8 and 5.4), MES (pH 5.8 and 6.2), MOPS (pH 6.6 and 7.0), HEPES (pH 7.4 and 7.8), and Glycine (pH 8.6 and 9.0) were used as the pH buffers. The p*K*a was determined by fitting the data to the sigmoidal dose-response equation.

**Measurement of photostability.** Fluorescent proteins expressed in HeLa cells were photobleached using a mercury arc-lamp–equipped TE2000E inverted microscope (Nikon) with an Apo-VC 40x, 1.30 NA oil-immersion objective (Nikon), and FF01-370/36), CFW-Di01-Clin, and FF01-435/40 (all from Semrock) as the excitation filter, dichroic mirror, and emission filter, respectively. Neutral density filters were removed, and fluorescence images of HeLa cells were taken every 10 sec with a 10-ms exposure time using a cooled CCD camera, ORCA-AG (Hamamatsu Photonics) under the control software, AquaCosmos (Hamamatsu Photonics). Laser photobleaching was